Atmospheric Environment 213 (2019) 159–169

Contents lists available at ScienceDirect

Atmospheric Environment

journal homepage: www.elsevier.com/locate/atmosenv

Performance of MODIS high-resolution MAIAC aerosol algorithm in China: Characterization and limitation

Minghui Tao[a,*], Jun Wang[b], Rong Li[c,**], Lili Wang[d], Lunche Wang[a], Zifeng Wang[e], Jinhua Tao[e], Huizheng Che[f], Liangfu Chen[e]

[a] Hubei Key Laboratory of Critical Zone Evolution, School of Geography and Information Engineering, China University of Geosciences, Wuhan, 430074, China
[b] Dept. of Chemical & Environmental Engineering, University of Iowa, Iowa City, 52242-1503, USA
[c] School of Resources and Environmental Science, Hubei University, Wuhan, 430062, China
[d] State Key Laboratory of Atmospheric Boundary Layer Physics and Atmospheric Chemistry, Institute of Atmospheric Physics, Chinese Academy of Sciences, Beijing, 100029, China
[e] State Key Laboratory of Remote Sensing Science, Institute of Remote Sensing and Digital Earth, Chinese Academy of Sciences, Beijing, 100101, China
[f] Key Laboratory of Atmospheric Chemistry, Chinese Academy of Meteorological Sciences, Beijing, 100081, China

ARTICLE INFO

Keywords:
Aerosols
MAIAC
Algorithm
MODIS
China

ABSTRACT

The MODIS Multiple Angle Implication of Atmospheric Correction (MAIAC) algorithm enables simultaneous retrieval of aerosol and bidirectional surface reflectance at high resolution of 1 km. Taking advantage of multi-angle and image-based information, the MAIAC algorithm has great potential for improving retrieval of aerosols over both dark and bright surfaces. Here, by comparing MAIAC aerosol products with the ground-based observations at 9 typical sites spread out in China, we gain the insights regarding the performance of MAIAC algorithm, for the first time, over Asia that has complicated surface types, diverse aerosol sources, and heavy loading of aerosols in the atmosphere. While aerosol products from MAIAC show similar spatial distribution as that from MODIS Dark-Target (DT) and Deep-Blue (DB) algorithms, they are superior to reveal numerous hotspots of high AOD values in fine scales due to their higher resolution at 1 km. Moreover, since MAIAC algorithm for cloud screening uses time series of observations, it shows higher effectiveness to mask cloudy pixels as well as the pixels of the melting and aging ice/snow surfaces. While MAIAC and ground-observed AOD values show high correlation coefficient of ~0.94 in two AERONET sites of Beijing and Xianghe, considerable bias is prevalent in other regions of China. Systematic underestimation is found over the deserts in western China likely due to the high bias of single scattering properties of aerosol model prescribed in MAIAC algorithm. In eastern China, the distinct positive bias is found in conditions with low-moderate AOD values and likely results from errors in regression coefficients in the surface reflectance model. Given its advantages in cloud and snow/ice screening and retrieval in fine spatial resolution, MAIAC algorithm can be improved by further refinement of regional aerosol and surface properties.

1. Introduction

Atmospheric aerosols play key roles in the Earth's climate and environmental systems through intricately interacting with solar radiation, clouds, and atmospheric chemistry (Charlson et al., 1992; Fan et al., 2018; Martin et al., 2003). Atmospheric aerosol particles can be originated from both human activities such as fossil fuel combustion and industrial emissions and natural processes such as fires, volcanic eruptions, and surface aeolian (wind-blown) activities. Both the amount and composition of aerosol particles often exhibit very inhomogeneous distribution from regional to global scales due to their short lifetime and diverse sources, exerting large uncertainties in climate research (IPCC, 2013). Therefore, global observation of aerosol properties with high spatiotemporal resolution and accuracy is a fundamental requirement toward further understanding of aerosol impacts on air quality and climate (Diner et al., 2018; Mishchenko et al., 2004).

Since the late 1990s, different algorithms have been used to retrieve aerosol properties globally from various well-calibrated satellite instruments (King et al., 1999). Because of many unknowns of aerosol and surface parameters that regulate the transfer of radiation at the surface

* Corresponding author. NO. 388, Lumo Road, Hongshan District, Wuhan, 430074, China.
** Corresponding author. NO. 368, Youyi Road, Wuchang District, Wuhan, 430062, China.
E-mail addresses: taomh@cug.edu.cn (M. Tao), rongli@hubu.edu.cn (R. Li).

https://doi.org/10.1016/j.atmosenv.2019.06.004
Received 5 November 2018; Received in revised form 30 April 2019; Accepted 1 June 2019
Available online 03 June 2019
1352-2310/

and in the atmosphere, satellite retrieval of aerosol optical depth (AOD) is a challenging work. In particular, the sensitivity of backscattered radiances at the top of the atmosphere (TOA) to the variations of aerosol properties is much weaker over visibly bright surfaces (such as deserts and urban regions) than dark surfaces. Ultraviolet, multi-angle, and polarization satellite sensors such as Ozone Monitoring Instrument (OMI), Multi-angle Imaging SpectroRadiometer (MISR) and POLarization and Directionality of Earth's Reflectance (POLDER) have advantages to derive aerosol properties because surface reflectance in UV and polarized surface reflectance are smaller than the counterparts in the visible spectrum (Diner et al., 2005; Dubovik et al., 2011; Torres et al., 2007). However, current satellite sensors with the capabilities of measuring UV or polarization often have coarser pixel resolution or narrower swath width or shorter data records when they are compared with MODerate Resolution Imaging Spectroradiometer (MODIS), thus making a considerable impediment in some applications.

MODIS instruments aboard Terra since 2000 and Aqua since 2002 respectively provide daily near global aerosol products operationally with a wide swath of ~2330 km at the ground (Hsu et al., 2013; Levy et al., 2013). The standard MODIS aerosol products are provided with two spatial resolutions, one at 10 km at nadir, and another at 3 km that was added in MODIS Collection (C) 6 for air quality studies (Remer et al., 2013). However, Lambertian land surface is assumed in MODIS Dark Target (DT) and Deep Blue (DB) algorithm, and surface anisotropy can result in uncertainties of aerosol retrievals (Lyapustin et al., 2011a). Recently, MODIS Multiple Angle Implication of Atmospheric Correction (MAIAC) algorithm enables simultaneous retrieval of aerosol loading and Bidirectional Reflectance Distribution Function (BRDF) parameters at high resolution of 1 km (Lyapustin et al., 2011b, 2018), providing excellent opportunity for aerosol research at finer spatial scales. Although MODIS MAIAC algorithm exhibits high accuracy in North and South America (Martins et al., 2017; Superczynski et al., 2017), its performance remains unclear in China due to few validation studies in the past, despite of high loading and complicated properties of aerosols in China (Tao et al., 2012, 2015).

The main purpose of this study is to present, for the first time, a comprehensive evaluation of and the insights therein the performance of the MAIAC algorithm in regions of heavy aerosol loading and diverse surface types in China. MODIS MAIAC retrievals are evaluated via ground-based validation across China with Sun photometers from Aerosol Robotic Network (AERONET) and Chinese Aerosol Remote Sensing Network (CARSNET). Inter-comparison of MODIS MAIAC aerosol products with operational C6.1 MODIS DT and DB aerosol products is conducted to examine characteristics of MAIAC retrieval in regional scale. In addition, the uncertainty and applicability of MAIAC algorithm in China are also discussed.

2. Data and methods

2.1. MODIS aerosol algorithms

To retrieve independent variables from the multi-spectral MODIS radiances that depend on atmosphere and surface properties as well as their coupling in radiative transfer, assumption or prior knowledge has to be used to constrain and simplify the problem of inversion or retrieval. The operational MODIS aerosol retrieval was first implemented by the Dark Target (DT) algorithm over surfaces of dense vegetation using assumed relationship in surface reflectance between visible and shortwave bands (Kaufman et al., 1997). Variation of aerosol single scattering properties is prescribed based on the AERONET climatology, and only regional-to-continental variations at seasonal scale are considered. Hence, the size distributions and refraction indices for both fine and coarse-mode aerosol particles are predefined in the generation of the lookup table (LUT) in which radiances at TOA are simulated as a function of the retrieval parameters such as aerosol optical depth (AOD) and fine-mode AOD fraction. For aerosol retrieval over bright surfaces such as deserts, MODIS Deep Blue (DB) algorithm establishes pre-calculated surface reflectance database in blue bands (412 and 470 nm) as a function of scattering angle, NDVI (Normalized Differential Vegetation Index), and season (Hsu et al, 2013; 2013). Moreover, in MODIS C6, DB retrieval has been extended to all snow/ice-free areas by utilizing spectral relationship of surface reflectance in vegetated region and considering angular shapes of surface BRDF in urban/croplands areas.

MAIAC is applied to the MODIS level 1B land-surface radiances that is generated for the sinusoidal grids at 1 km resolution globally. Subsequently, to simultaneously retrieve aerosol and surface parameters, MAIAC algorithm utilizes multi-angle information from time series of MODIS observation for up to 16 days for a given pixel at the resolution of 1 km (Lyapstin et al., 2011b). With the spectral similarity assumption for BRDF shape, a spectral regression coefficient (SRC) can be used to relate bidirectional reflectance factors (BRF) at blue to shortwave band at 2.1 μm; the latter band is usually considered as atmospherically transparent except in dusty conditions (Wang et al., 2010). Started for the North America, the C6 MAIAC algorithm has been expanded recently to the global land surfaces with considerable changes, and improved several key components including snow/ice screening, SRC estimation and aerosol properties (Lyapstin et al., 2018). Since SRC determination using multiday minimization method within 25 × 25 km can lead to discontinuity in block edges, the C6 MAIAC utilizes minimal ratio of spectral reflectance (0.47/2.13 μm) in 2-month period to estimate SRC at 1 km pixel level, which is similar as that used in Wang et al. (2010). Instead of retrieving fraction of fine/coarse aerosols, eight aerosol models are prescribed to different regions of the world to represent corresponding aerosol types. China is mainly covered by two aerosol models: industrial aerosol model derived from AERONET site of Beijing for the whole eastern China, and the same aerosol model considering contribution of dust particles in western USA for western China.

The current C6.1 MODIS aerosol products provide DT AOD data at two spatial resolutions of 10 km and 3 km respectively at nadir, and DB aerosol data at 10 km. Ground validation shows that ~2/3 global MODIS DT retrievals fall within expected error envelope of ± ($15\%AOD_{AERONET} + 0.05$) (Levy et al., 2013). However, DT AOD retrievals exhibit obviously systematic overestimation in eastern China, which is dominated by improper aerosol models and bias in surface reflectance estimation in urban regions (Tao et al., 2015; Wang et al., 2010). There has been some improvement in estimation methods of urban surface reflectance since C6.1 MODIS aerosol algorithm (Gupta et al, 2018). By contrast, MODIS DB retrievals perform well in eastern China, but obviously underestimate aerosol loading in deserts of western China (Tao et al., 2017a). The C6 MODIS MAIAC aerosol products has strict screening for pixels possibly cloudy and adjacent to clouds (Lyapstin et al., 2018). We utilize C6.1 MODIS 3 km DT, 10 km DB, and C6 MAIAC 1 km AOD for inter-comparison, in which only retrievals of best quality are selected. The MAIAC data used for this analysis in China region was obtained from NASA released in May 2017 (https://portal.nccs.nasa.gov/datashare/maiac/).

2.2. AERONET and CARSNET measurements

AERONET is a global ground-based remote sensing network of Sun photometers providing highly accurate measurements and inversions of aerosol optical and microphysical properties (Holben et al., 1998; Giles et al., 2019). By direct sun observations of Sun photometers, spectral AOD can be determined in 10–15 min intervals with very low uncertainties ~0.01–0.02 (Eck et al., 1999). Combined with spectral AOD, sky light measurements in almucantar mode enable reliable inversion of aerosol physical properties such as size distribution and refractive index (Dubovik et al., 2000). Although the refraction index is assumed to be independent of particle size in the AEROENT inversion, this assumption is needed because the measurements of sky radiances

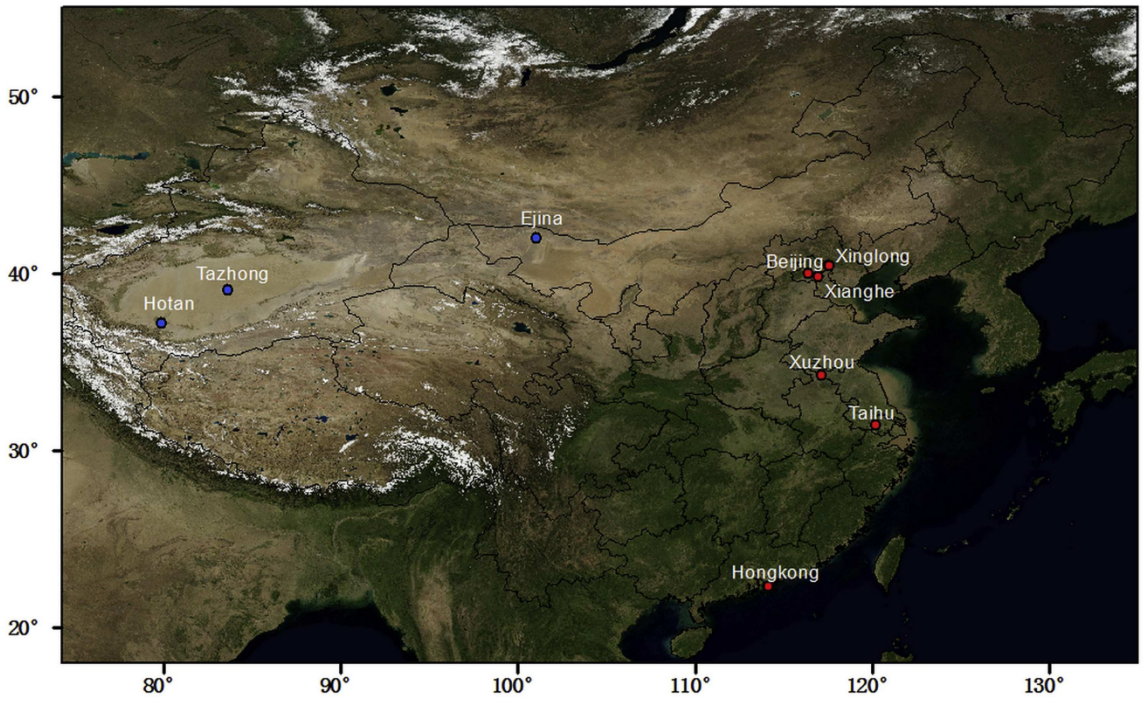

Fig. 1. a) Geographic location of AERONET sites (red) and CARSNET sites (blue) in MODIS true color image of mainland China. (For interpretation of the references to color in this figure legend, the reader is referred to the Web version of this article.)

alone are not sufficient for separate inversion of refraction index for both fine and coarse particles (Xu and Wang, 2015), and future AEROENT sensors with measurements of sky light polarization may be helpful to alleviate this assumption (Xu et al., 2015). The AERONET aerosol products have consistent cloud screening and quality control procedures in Level (L) 1.5, and quality-assured check with post-filed calibration in L2.0.

Since CARSNET follows closely with AEORENT's instrumentation and measurement protocol, it has similar accuracy of the spectral AOD in China as that of AERONET (Che et al., 2009). Established in 2002 with continuous updates in last several years, CARSNET also use the similar protocol as AERONET in terms of data collection and calibration. As shown in Fig. 1, we combined AERONET and CARSNET at a total of 9 sites with available observations during 2003–2016 to evaluate performance of MAIAC algorithm in typical surface types such as urban, rural areas, mountain and deserts.

To have a cross-examination of the performance of current C6 MODIS MAIAC retrievals, we used recent C6.1 MODIS 3 km DT and 10 km DB aerosol products for inter-comparison, which has been compared against ground-based observations and showed well-quantified accuracy (Gupta et al., 2016; Tao et al., 2015). Ground validation of MAIAC aerosol algorithm is conducted by using Level 2 AERONET and CARSNET AOD data after calibration. However, for those sites such as Xuzhou site that has fewer or don't have L2.0 products, L1.5 data is selected. Since Sun photometers do not have 550 nm bands, spectral AODs at neighboring bands of 550 nm are interpolated with standard Ångström exponent.

To match satellite retrieval with ground measurements, collocation methods with spatial and temporal average are adopted (Ichoku et al., 2002). Validation of MODIS 10 km aerosol products usually chooses a spatial radius of 25 km for satellite pixels with selected site centered in and a temporal interval of ± 30 min of satellite passing time for ground observations (Levy et al., 2013; Anderson et al., 2013). Some validations such as MODIS 3 km AOD adopt smaller radius (Gupta et al, 2018), but sensitivity test shows that spatial and temporal window sizes within the same order have no obvious influence on correlation of the matchups (Martins et al., 2017). To facilitate inter-comparison with MODIS aerosol retrievals, here we utilize consistent collocation approach with matched satellite pixels in 25 km radius and ground observations in ± 30 min interval. Considering that the few available retrievals in cloudy or snow/ice conditions may not well represent overall AOD within the spatial radius, such daily matchup is discarded if fraction of selected satellite pixels with valid retrievals is < 20%.

3. Results and analysis

3.1. Overall inter-comparison of MODIS aerosol products

Fig. 2 shows spatial variations of MODIS 1 km MAIAC, 3 km DT and 10 km DB AOD on one clear day of summer in northern China. Compared with the MODIS DT and DB aerosol products, the most striking feature of MAIAC AOD is the fine-scale characterization of the hotspot pixels with high aerosol loading such as small towns, which likely reflects numerous sources of emissions at local scale. Despite abundant vegetation during summer in northern China, the MODIS 3 km DT retrievals are unavailable in most urban regions due largely to insufficient dark pixels (Fig. 2c). There is a generally similar spatial distribution between MAIAC and DT AOD, but the DT AOD values are lower. Moreover, because 10 km DB AOD product misses most of the hotspots of high aerosol loading, its values are lower than MAIAC results. Considering the distinct difference of MAIAC aerosol retrievals with respect to the current MODIS aerosol products, accuracy and uncertainties of MAIAC algorithm are quantified below.

To have an overview of different MODIS aerosol products in China, annual mean of AOD values retrieved respectively from MAIAC, DB, and 3 km DT algorithms and their corresponding sampling frequency are displayed in Fig. 3. Both MAIAC and DB algorithm retrieve aerosol properties over cloud-free and ice/snow-free land surfaces, but their results exhibit clear differences. It is worth noting that annual mean of MAIAC AOD values is lower than that of DB in northeastern China and northern part of northern China, and higher in most of the other areas. Frequency of available annual retrievals of DB AOD is higher than that

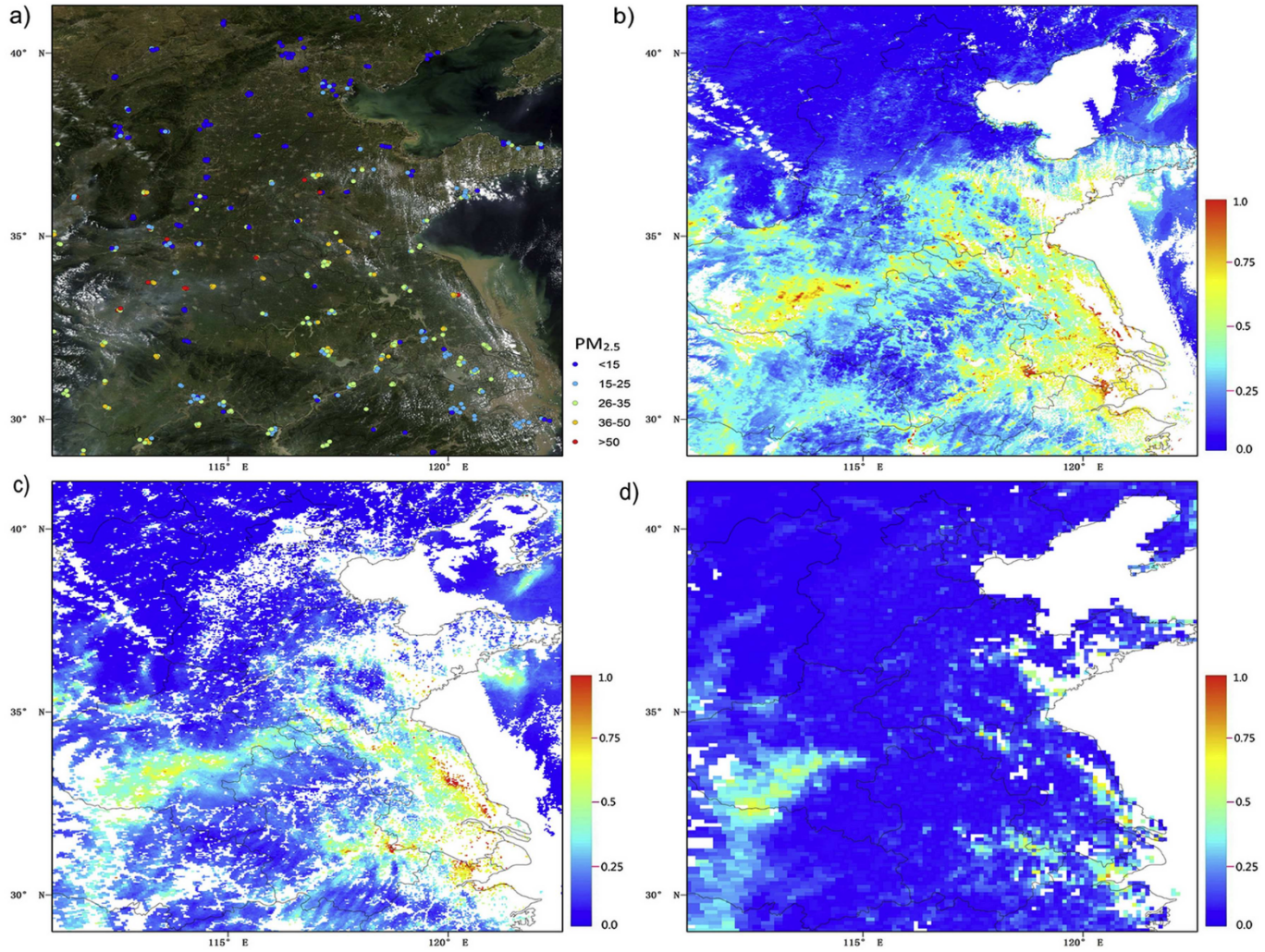

Fig. 2. a) Hourly concentration of $PM_{2.5}$ in Aqua MODIS true color image, b) MODIS MAIAC 1 km AOD, c) DT 3 km AOD, d) DB 10 km AOD on August 28, 2016. (For interpretation of the references to color in this figure legend, the reader is referred to the Web version of this article.)

of MAIAC except in the Tibetan Plateau, which is caused by different cloud mask methods and pixel aggregation of 10 km DB retrieval. It should be noted that C6 MAIAC algorithm does not retrieve AOD at high elevation (> 4.2 km), and assumes a low climatology AOD ~ 0.02 instead (Lyapstin et al., 2018). Therefore, the fixed low AOD over Tibetan Plateau and its associated high frequency result from climatological value in MAIAC. By contrast, annual available retrievals of 3 km DT AOD are ~1/3 of these of MAIAC and DB, which can largely limit its application to study Particulate Matter (PM) air quality due to the poor temporal representativeness and spatial coverage.

To make a further inspection of the difference between MAIAC retrievals and well validated DB AOD product, a pollution day typical in winter in eastern China was selected (Fig. 4). Regional haze pollution is prevalent during the coal burning period in winter (Tao et al., 2012). Although both MAIAC and DB AOD values are higher in areas that show the gray haze plumes in MODIS true color image, their magnitude differ significantly from their corresponding annual mean values. It can be seen that MAIAC AOD values around Beijing and in northeastern China are obviously lower than DB AOD results. Conversely, MAIAC AOD values get much higher than DB retrievals in the south of ~38°N. In particular, MAIAC AOD shows prevalent high values (~0.7) around rectangle B in Fig. 4b, about twice of the DB values (~0.3).

Another prominent contrast in Fig. 4 is the spatial coverage of different MODIS AOD products. The area of high AOD values in DB product (denoted as rectangle A at the top of Fig. 4c) is not available in MAIAC retrievals (Fig. 5b), because it was confirmed as snow region by MAIAC algorithm. Unlike the strict cloud mask scheme of MAIAC algorithm, the very high AOD values in DB in the region with melted snow can be caused by failure of ice/snow screening in DB algorithm (Fig. 5c). Cloud screening of DB depending on threshold values of spectral radiance and their calculation is more sensitive to white snow. On the other hand, removal of pixels adjacent to cloud/snow leads to smaller area of MAIAC AOD than that of DB (Fig. 5e and f). The slightly lower frequency of MAIAC AOD retrievals can be mainly caused by its strict removal of pixels adjacent to clouds.

3.2. Ground validation of MODIS MAIAC aerosol algorithm

Fig. 6 shows the validation of MODIS MAIAC AOD in different regions of China. There is an obvious spatial difference in uncertainties of MATAC retrievals. Consequently, performance of MAIAC retrievals in China can be separated into three cases. First, most of MAIAC AOD values fall within expected error envelop of ± ($20\%AOD_{AERONET} + 0.05$) around Beijing, Xianghe, and Xinglong, but satellite retrievals get very scattered with larger bias in conditions of high AOD (> 1.0). Second, obvious overestimation of MAIAC AOD prevails in Xuzhou, Taihu, and Hongkong sites, which spreads across most part of eastern China. In contrast, aerosol loading in the deserts of western

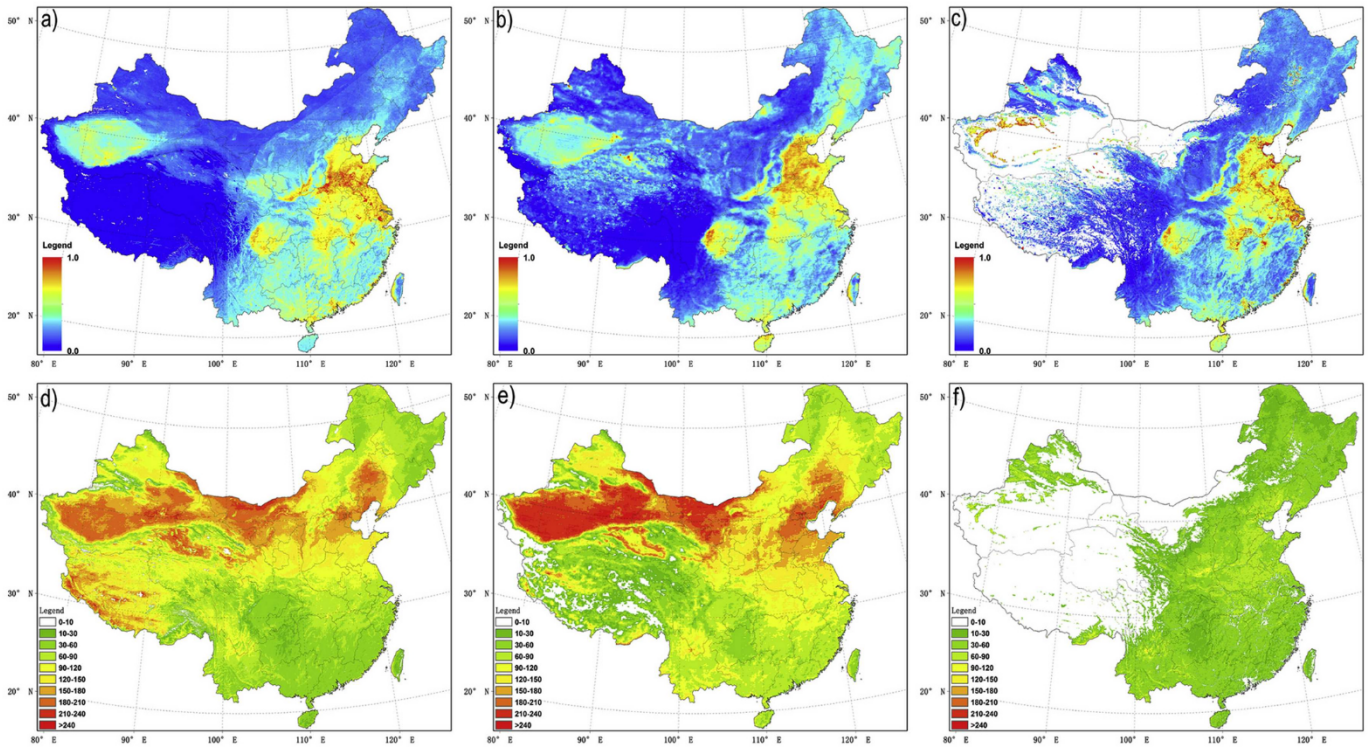

Fig. 3. Annual mean AOD (top) and its sampling frequency (bottom) respectively for a, c) MODIS MAIAC 1 km AOD, b, d) DB 10 km AOD, c, f) DT 3 km AOD of 2016.

China is widely underestimated. There is a notable systematic underestimation in low-moderate AOD values of MAIAC retrievals in Hotan and Tazhong of Taklimakan Desert, and such low bias disappear in conditions with high AOD values. Moreover, ground validation in Ejina shows much larger underestimation for MAIAC AOD in the Gobi deserts.

To enhance inter-comparison of MODIS aerosol algorithms, uncertainties of DB and DT AOD are also evaluated by ground validations (Figs. 7 and 8). DB retrievals show similar performance as MAIAC in Beijing, Xianghe, and Xinglong. Unlike the prominent overestimation of MAIAC AOD in Xuzhou, Taihu, and Hongkong, DB AOD values in eastern China mostly fall within the expected error envelop of $\pm$ ($20\%AOD_{AERONET}+0.05$) except underestimation of some retrievals in Hongkong. However, DB retrievals has much lower accuracy in western China with numerous abnormally-low AOD values (Tao et al., 2017a). By comparison, DT retrievals display good accuracy in Xianghe and Hongkong (Fig. 8), but they have considerable overestimation in low-AOD conditions in urban sites of Beijing and in moderate-high AOD (> 0.5) conditions in Xuzhou and Taihu. Although each aerosol algorithm has its own uncertainties, inter-comparison with

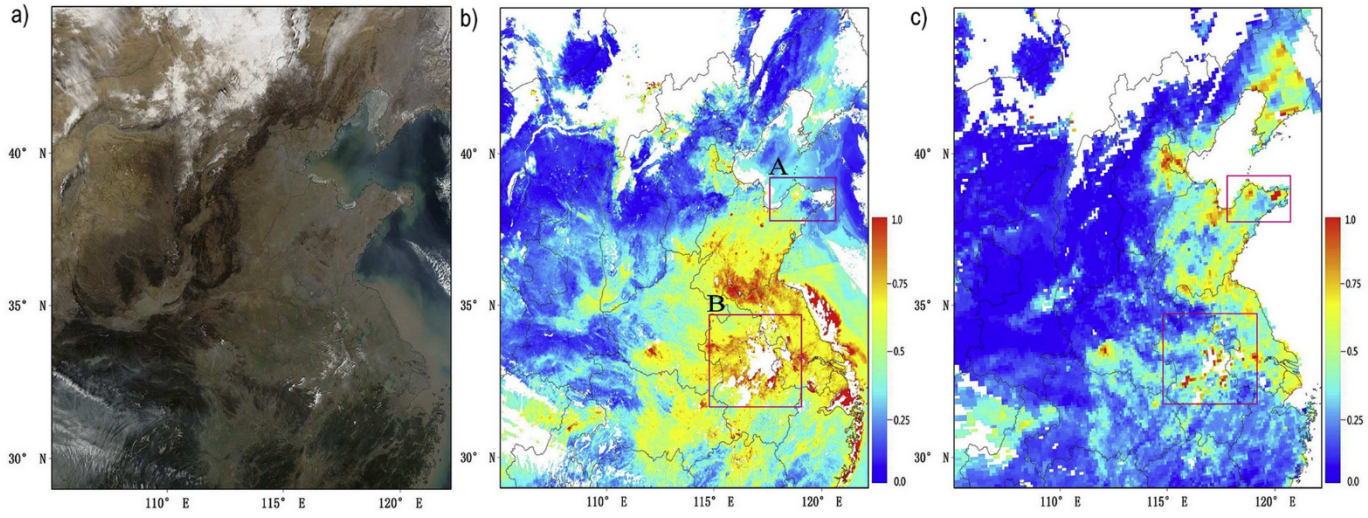

Fig. 4. a) Aqua MODIS true color image, b) MODIS MAIAC 1 km AOD, c) 10 km DB AOD over eastern China on February 7, 2016. The rectangles denote regions with obvious difference in AOD values and AOD spatial coverage. (For interpretation of the references to color in this figure legend, the reader is referred to the Web version of this article.)

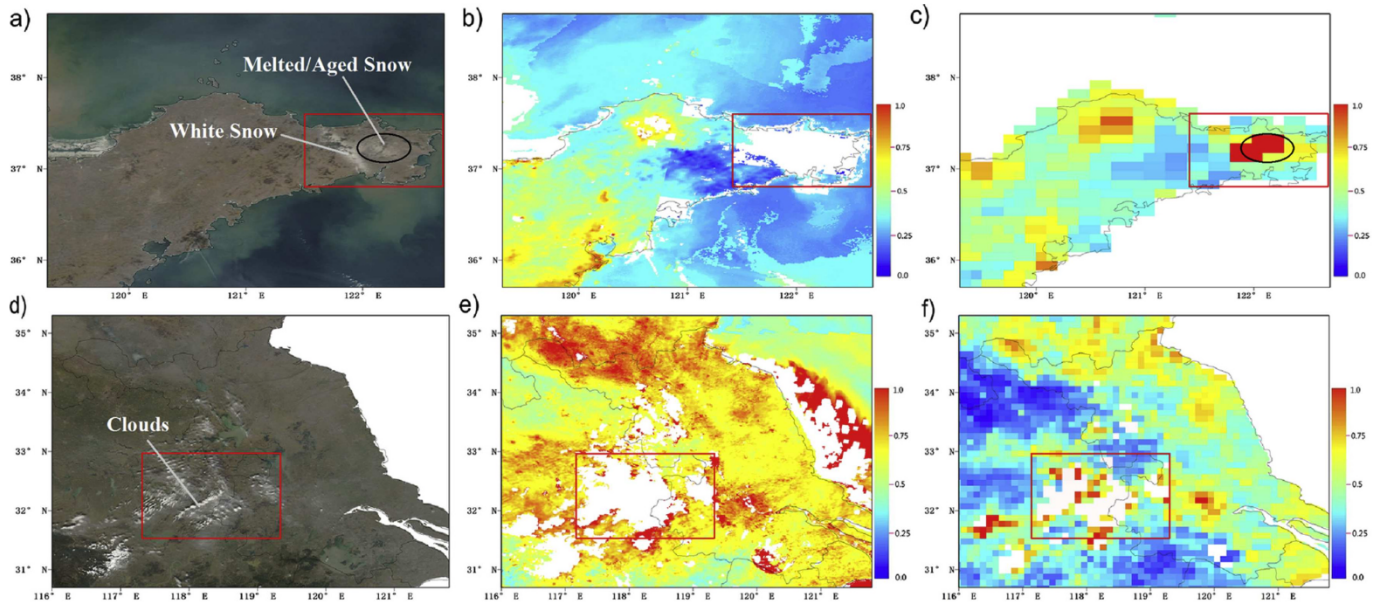

Fig. 5. Same as Fig. 4 but for specified regions of the rectangle in Fig. 4.

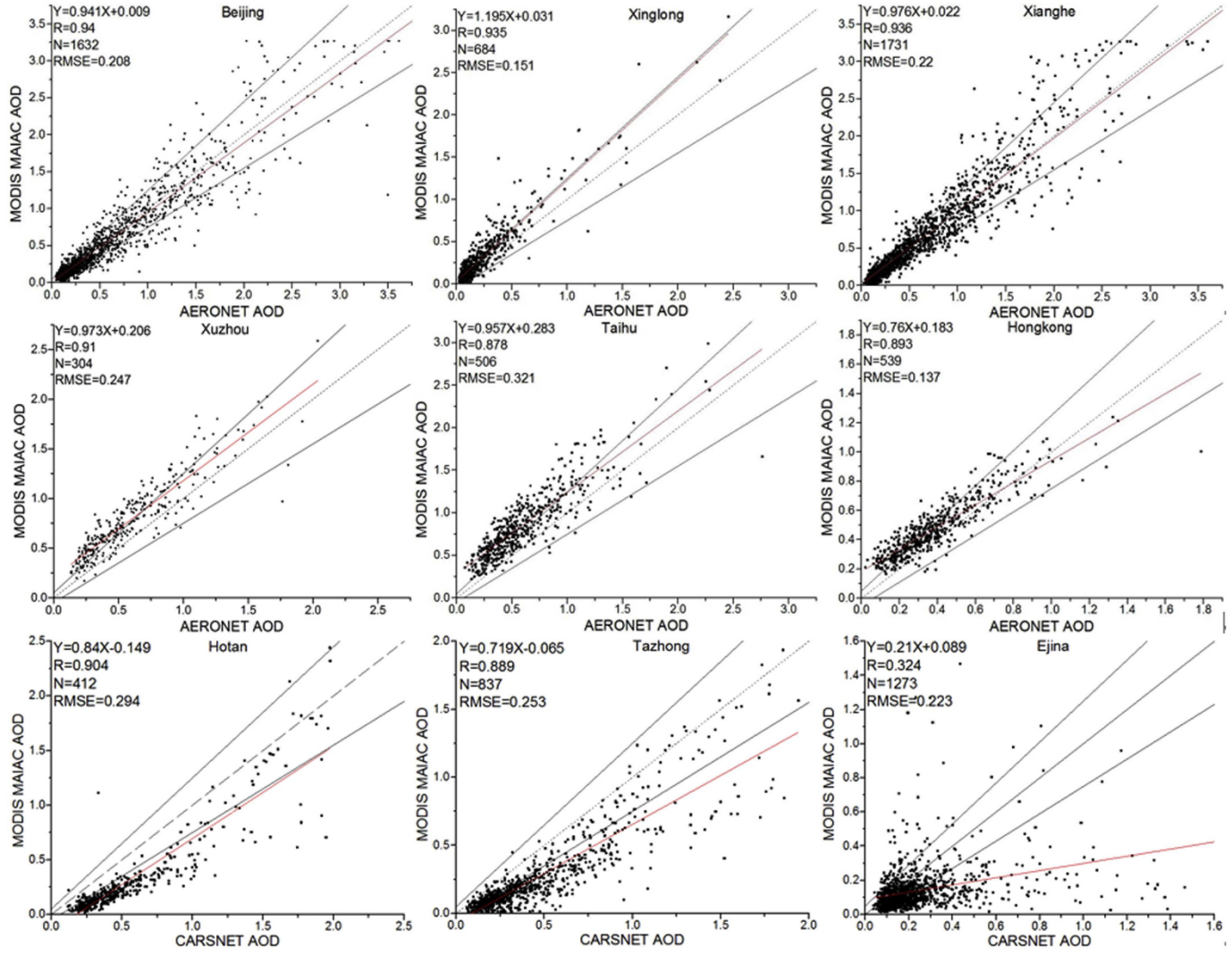

Fig. 6. Scatter plots of MODIS MAIAC 1 km AOD at 550 nm compared with AERONET or CARSNET measurements in typical surface types of China. The red, black and dotted lines indicate their linear fitting, ± (0.05 + 20%) of the AERONET AOD, and 1:1 line, respectively. (For interpretation of the references to color in this figure legend, the reader is referred to the Web version of this article.)

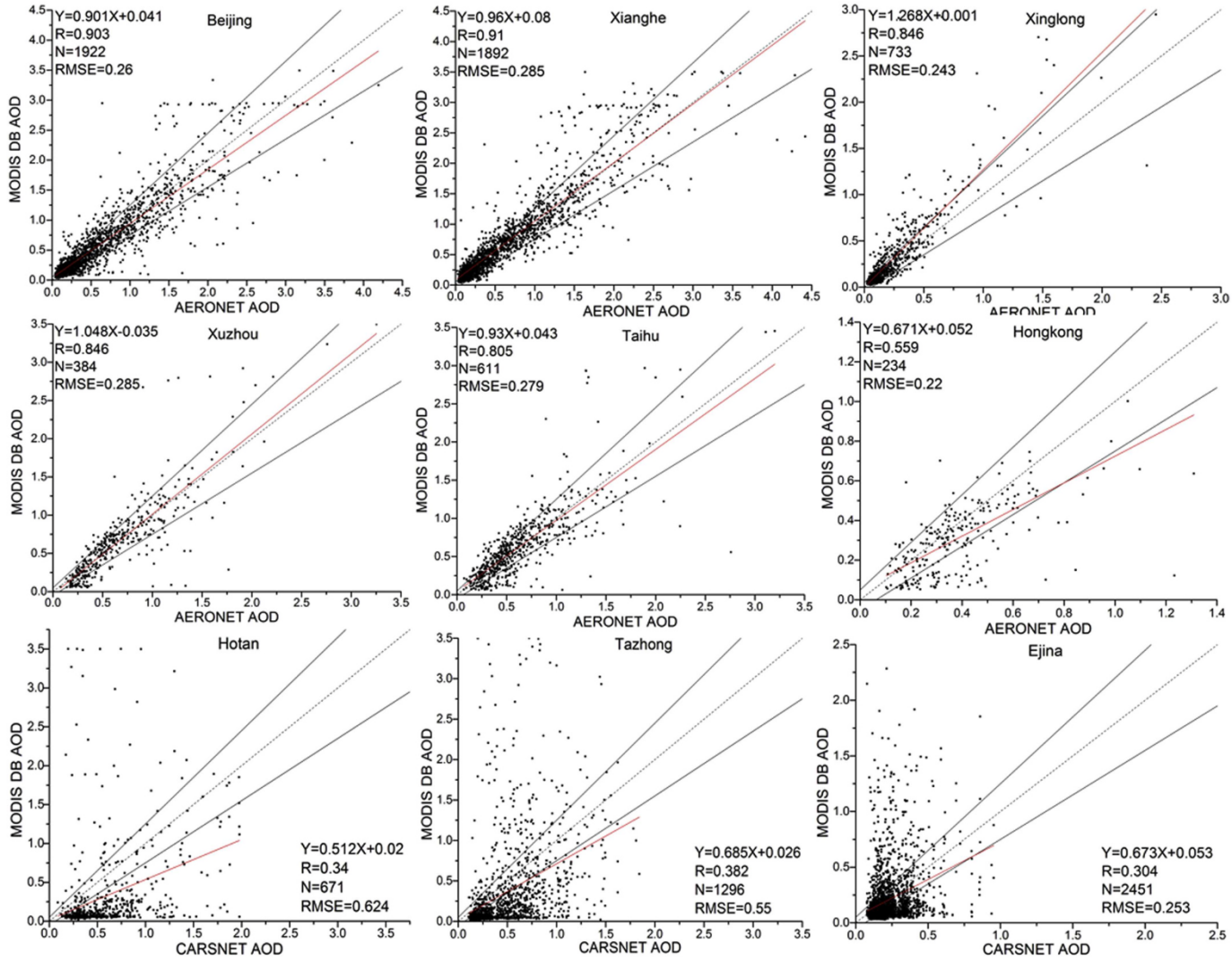

Fig. 7. Same as Fig. 6 but for Collection 6.1 MODIS DB 10 km AOD.

DB and DT retrievals provides a regional insight into strengths and weaknesses of MAIAC algorithm.

The dependence of MAIAC AOD bias on true AOD values exhibit distinct patterns in different season and regions (Fig. 9). Despite their normal distribution centered around zero, MAIAC AOD errors in Beijing and Xianghe show obvious seasonal changes with respect to ground-based AOD. Considering that only one fixed aerosol model is used in eastern China throughout the whole year, MAIAC AOD is generally overestimated in summer and underestimated in winter. While centered close to zero, the envelop of error spread gets larger as AOD values get larger, but such dependence is opposite when AOD is higher than 2.0. MAIAC retrieval errors in the mountain site of Xinglong monotonically increase with AOD. Although notable overestimation (positive bias) is predominated for MAIAC retrievals in Xuzhou, Taihu, and Hongkong, there is a clear decline in MAIAC retrieval bias as AOD increases. Contrary to its performance in eastern China, MAIAC AOD product shows large underestimation (negative bias) over the deserts of western China without notable seasonal dependence.

To further examine performance of different aerosol algorithms, collocated daily AOD values from AERONET, MODIS DB, and MAIAC retrievals are compared in Beijing and Xuzhou during 2016 (Fig. 10). Consistent with ground validation in Beijing, both DB and MAIAC AOD accurately capture the variations of the daily aerosol loading except several abnormal high cases in DB values, which can be caused by heavy haze plumes in the edge of matchup box (Tao et al., 2015). While MODIS DB retrievals in Xuzhou perform well as in Beijing, prevalent overestimation appears in MAIAC AOD values. The strong dependence of MAIAC AOD bias on seasonal and geographical location indicates improper assumptions for aerosol or surface models.

3.3. Source of uncertainties of MODIS MAIAC algorithm in China

Statistical correlation between satellite AOD and ground observations is the most common way to analyze error sources of aerosol retrieval algorithms (Anderson et al., 2013; Levy et al., 2013; Tao et al., 2015). Past studies have revealed that the slope and the intercept of the linear fit of AOD values between retrieved (y) and ground truth (x) indicate respectively the extent to which aerosol model assumption and surface reflectance estimation are accurate in the retrieval algorithm; the slope close to 1 and the intercept close to 0 suggest the good validity of assumptions made for the retrieval. As shown in Figs. 6 and 9, the low slope (0.21–0.84) of MAIAC validation in the deserts of western China demonstrates obvious systematic overestimation of aerosol scattering ability in MAIAC aerosol model, which is also one important source of MODIS DB AOD errors (Tao et al., 2017a). By contrast, positive bias of MAIAC AOD in Xuzhou, Taihu, and Hongkong is higher in low-moderate values, and gets lower as aerosol loading increases. Slight errors in surface reflectance estimation can cause large retrieval bias in

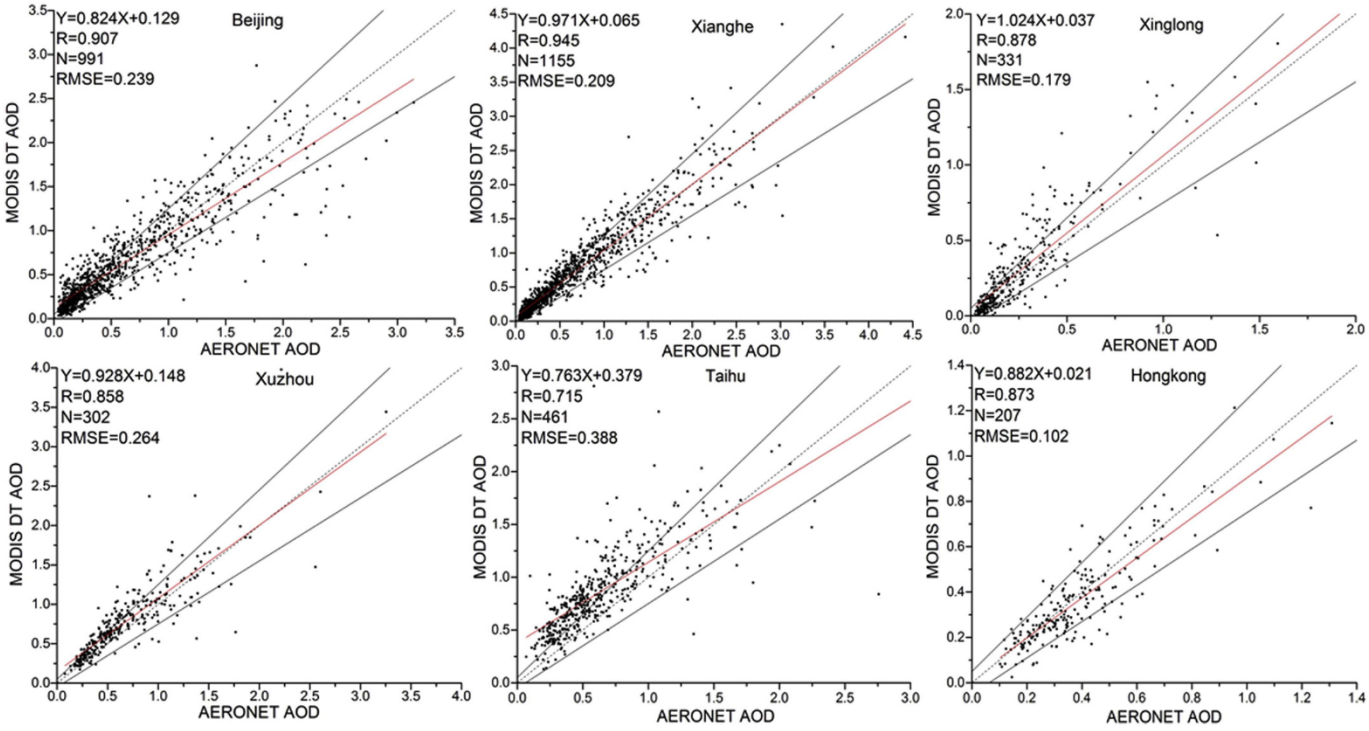

Fig. 8. Same as Fig. 6 but for Collection 6.1 MODIS DT 10 km AOD. Comparison with ground observation in desert site is not shown due to few available DT retrievals.

low-moderate AOD conditions, and influence of surface noise declines as aerosol loading becomes larger. How, it remains unclear why overestimation of MAIAC AOD associated with surface reflectance error in eastern China does not appear in Beijing and Xianghe, because the surface types in these regions and other parts in east China have similar surface types.

Fig. 11 shows the variations of MAIAC AOD bias with estimated surface reflectance, aerosol size, and scattering angle. In Beijing, these factors and retrieval errors show no obvious correlation. Surprisingly, MAIAC AOD bias in Xuzhou does not change with estimated surface reflectance as MODIS DT and DB retrieval errors (Tao et al., 2015, 2017a). Instead, MAIAC retrieval bias increases with Ångström exponent of AERONET AOD. It should be noted that SRC used for calculation of surface reflectance at 0.47 μm is determined from minimal value of spectral 0.47/2.13 μm reflectance ratio in 1–2 month period. Considering that the predominant deciduous vegetation and cropland in eastern China have fast temporal changes in vegetation density, surface contribution can be underestimated by minimal SRC in transitional regions (Hsu et al., 2013). To tackle this issue, Wang et al. (2010) used the 5-day running mean of the slope in the linear fit between 0.47 μm and 2.13 μm MODIS TOA reflectance in 40 days as the 0.47/2.13 μm surface reflectance ratio for the retrieval on the day that is centered in 40 days. Moreover, coarse dust particles can affect the radiative transfer at 2.1 μm. Hence, in dusty days, correcting the dust effect at 2.1 μm is needed to derive surface reflectance at 0.47 μm from TOA reflectance at 2.1 μm (Wang et al., 2010). However, such correction requires the knowledge of the dust AOD fraction (Wang et al., 2010) that is not obtained in MAIAC algorithm because it assumes a constant AOD fraction. In addition, aerosol single scattering albedo from Xuzhou to southern China is larger than that in areas around Beijing and Xianghe (Tao et al., 2017b). Slight underestimation of SRC can lead to considerable bias in calculation of SRC, which then causes overestimation at 1 km aerosol retrieval by error propagation. In addition, MAIAC AOD bias increases within scattering angle of 80° and 130° due to longer slant path of aerosol scattering in large viewing angles.

Although seasonal aerosol models are utilized in MODIS DT and DB retrievals, they might be insufficient to describe the large variation of aerosol properties due to the diverse sources of aerosol emissions and dynamic weather patterns in China (Tao et al., 2017b). Fig. 12 shows daily variations of mean values of available MAIAC AOD bias and collocated AERONET AOD in Beijing and Xuzhou. Consistent with Fig. 9, MAIAC AOD bias in Beijing turns from slightly negative to positive in summer, which is largely due to deviation of fixed aerosol model to seasonal changes. Furthermore, Fig. 9 indicates that the actual daily bias has dramatic fluctuation in Beijing and Xianghe, where regional transport and floating dust prevail (Tao et al., 2012). By contrast, there is no obvious time dependence for MAIAC retrieval errors in Xuzhou and Hongkong. In particular, MAIAC AOD bias is distinct only in conditions with low-moderate AOD values (and not for conditions with large AOD values), indicating that retrieval errors mainly result from inappropriate assumption used in SRC estimation. Generally, MAIAC algorithm displays an excellent performance in China in comparison with that of MODIS DB and DT products. However, the inhomogeneous distribution of aerosol and surface properties in eastern China impacts obviously the accuracy of MAIAC retrievals, which should be considered in regional scales.

4. Conclusions

Recent C6 MODIS MAIAC algorithm enables retrieval of AOD and BRDF over both dark and bright surfaces at high resolution of 1 km, which has great application potential for air quality studies. However, satellite aerosol retrievals are usually subjected to considerable uncertainties in China that is characterized by high aerosol loading and diverse emission sources. To gain insights of the performance of MAIAC algorithm in such complicated background, ground-based validation with AERONET and CARSNET and inter-comparison with MODIS DT and DB retrievals were conducted in this study.

It is shown that MAIAC AOD values exhibit high accuracy in Beijing and Xianghe, but have prevalent biases in other regions. There is an obvious overestimation in low-moderate values of MAIAC AOD in

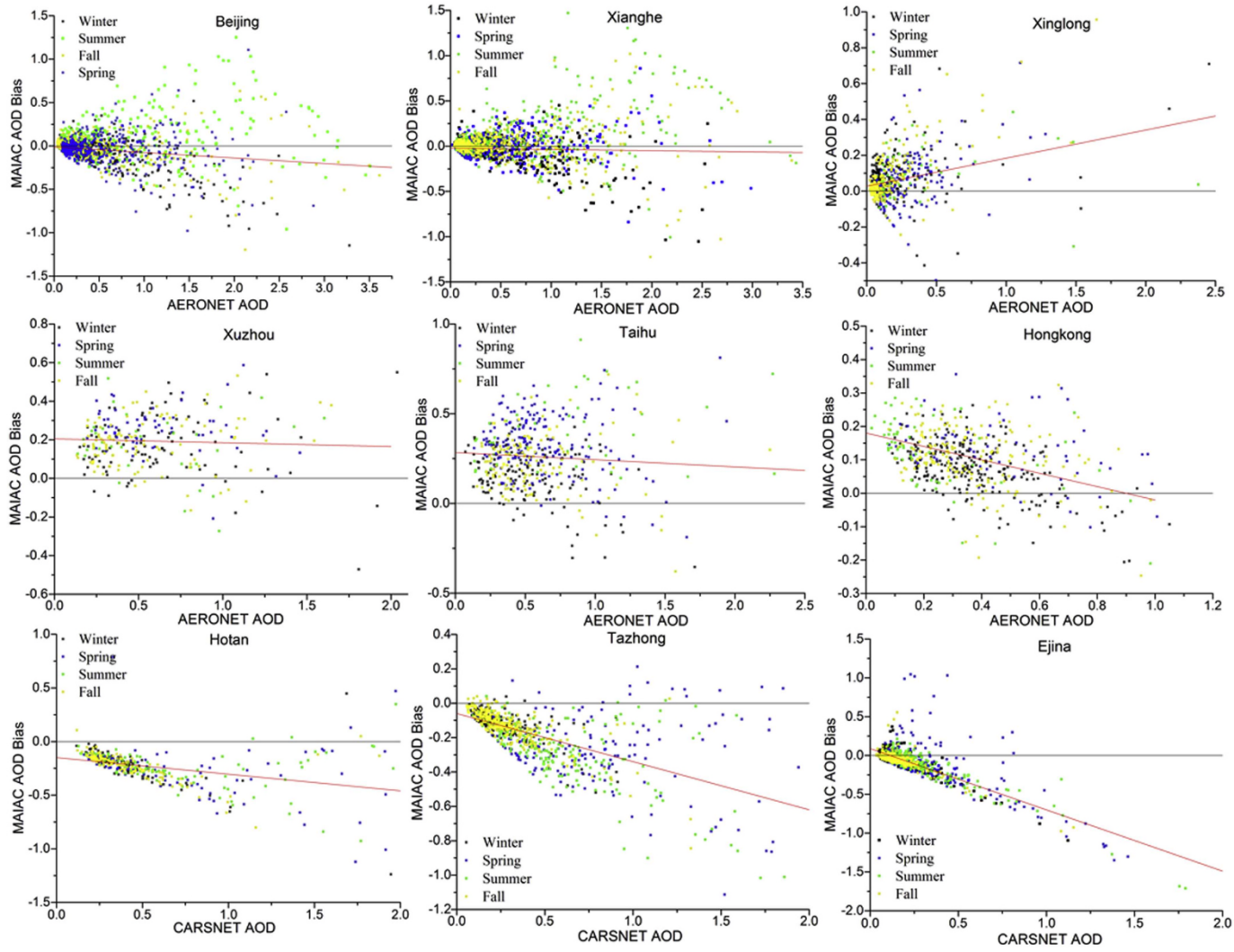

Fig. 9. Scatter plots of the difference between MAIAC retrieved and ground measurement AOD as a function of AERONET AOD. The black, blue, green, and yellow scatter represents winter, spring, summer and fall respectively, and the red line denotes linear fitting of all the values. (For interpretation of the references to color in this figure legend, the reader is referred to the Web version of this article.)

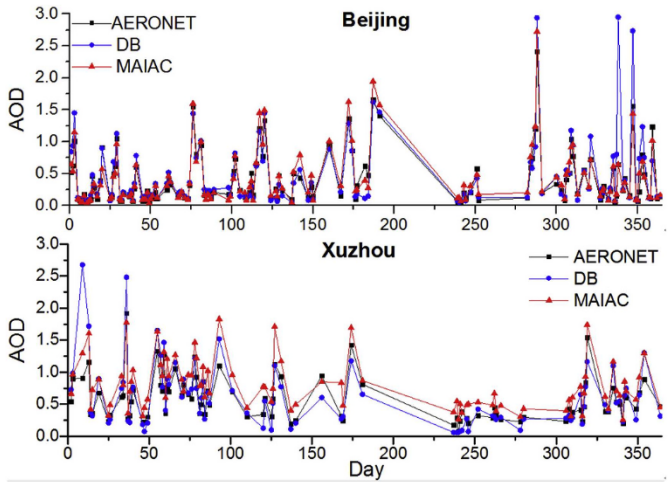

Fig. 10. Comparison of collocated MODIS MAIAC, DB, and ground-based AOD in Beijing and Xuzhou during 2016.

eastern China, and systematic underestimation dominates MAIAC retrievals over western China. Comparison with MODIS DB and DT products further confirms these findings for the MAIAC AOD products. Systematic negative bias demonstrates that MAIAC algorithm obviously overestimates single scattering properties of dust particles in northwestern China. Furthermore, SRC assumption could lead to underestimation of surface reflectance and subsequently propagates to 1 km aerosol retrieval.

In general, the uncertainties in surface SRC and aerosol model are two major error sources of MAIAC AOD in China. Given that aerosol sources are diverse and have strong seasonal and regional dependences, the aerosol single scattering properties derived from AEROENT sites around Beijing and western USA may not be applicable to regions in eastern and western China. Future studies are recommended to improve SRC calculation and assumption of aerosol properties in satellite retrieval algorithms with the data from more recent ground-based observation in eastern and western China. Considering the striking advantage in cloud and snow/ice screening, spatial coverage, and pixel resolution, MAIAC algorithm has the great potential for enhancing aerosol retrieval in China by improving its assumption of surface reflectance model and aerosol properties in regional scales.

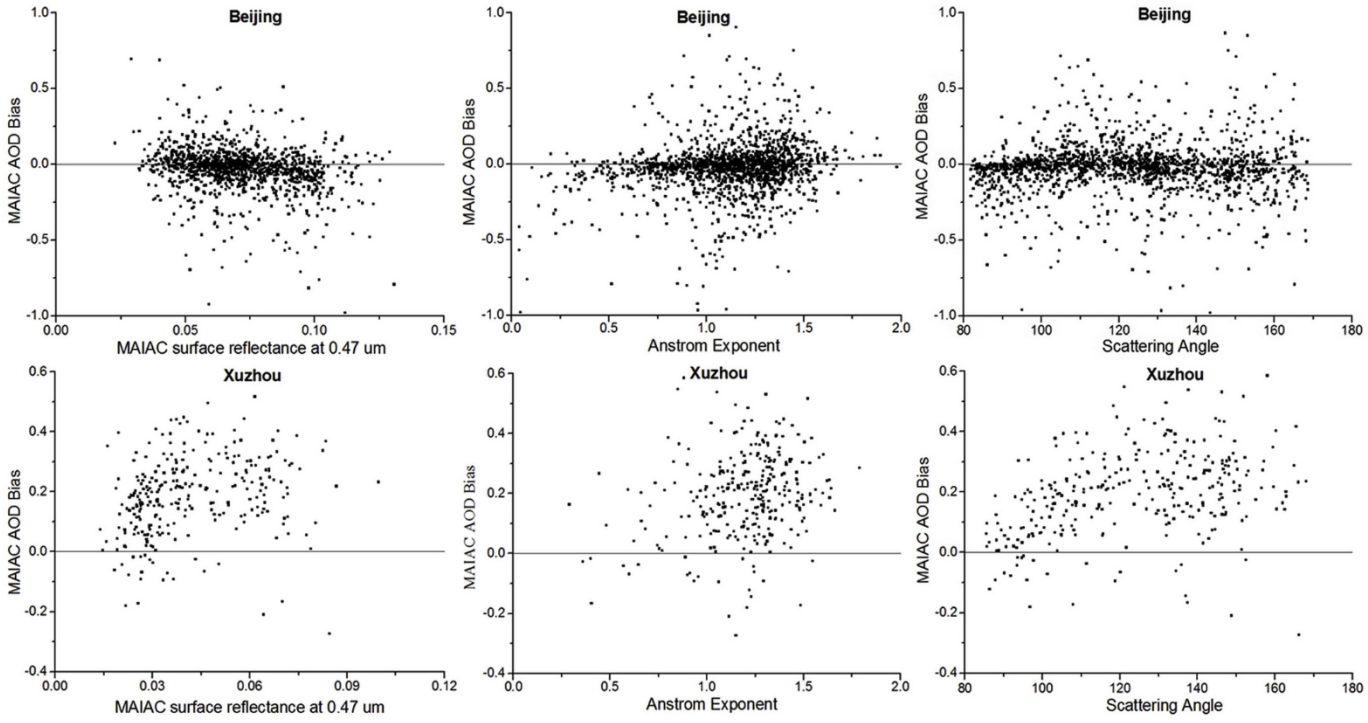

Fig. 11. MAIAC AOD bias as function of MAIAC surface reflectance at 470 nm, Ångström Exponent of AERONET AOD, and MAIAC scattering angle in Beijing (top) and Xuzhou (bottom).

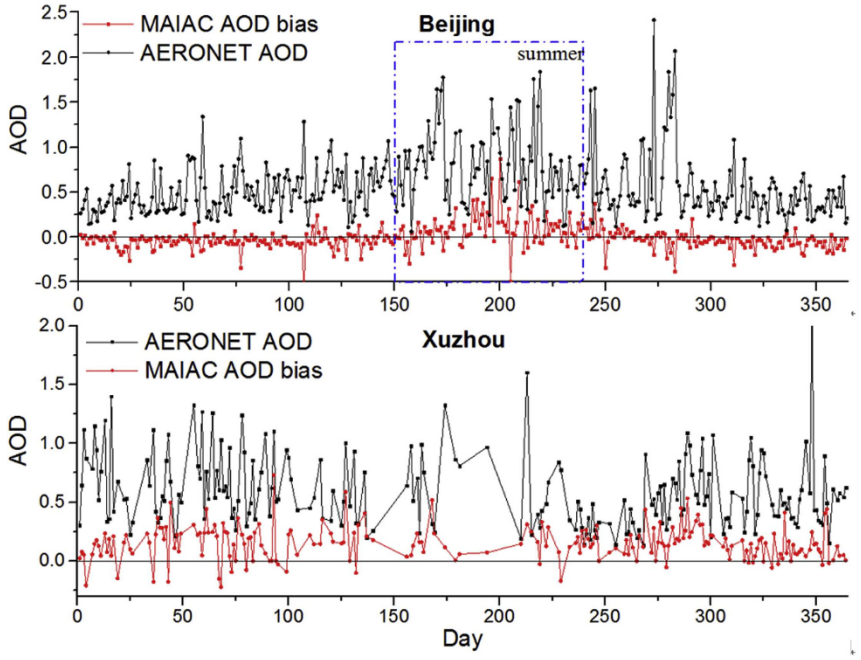

Fig. 12. Variations of mean values of available MODIS MAIAC AOD bias and collocated AERONET AOD in Beijing (2003–2016) and Xuzhou (2013–2016).

Acknowledgments

This study was supported by National Key R&D Program of China (Grant No. 2017YFB0503901) and National Science Foundation of China (Grant No. 41601472, 41871262, 41830109, 41471306). We thank the MODIS MAIAC team (https://portal.nccs.nasa.gov/datashare/maiac/) for the data used in our work. We acknowledge AERONET site PIs (B.N. Holben, H. Chen, L. Wu, R. Ma, J.E. Nichol, P. Wang, X. Xia, and Z. Li) for providing the aerosol data available.

Appendix A. Supplementary data

Supplementary data to this article can be found online at https://doi.org/10.1016/j.atmosenv.2019.06.004.

References

Anderson, J.C., Wang, J., et al., 2013. Long-term statistical assessment of Aqua-MODIS aerosol optical depth over coastal regions: bias characteristics and uncertainty sources. Tellus B: Chem. Phys. Meteorol. 65 (1), 20805.

Charlson, R.J., Schwartz, S.E., Hales, J.H., Cess, R.D., Coakley Jr., J.A., Hansen, J.E., Hofmann, D.J., 1992. Climate forcing by anthropogenic aerosols. Science 255, 423–430.

Che, H., et al., 2009. Instrument calibration and aerosol optical depth validation of the China Aerosol Remote Sensing Network. J. Geophys. Res.: Atmosphere 114, D03206. https://doi.org/10.1029/2008JD011030.

Diner, D.J., et al., 2005. The value of multiangle measurements for retrieving structurally and radiatively consistent properties of clouds, aerosols, and surfaces. Rem. Sens. Environ. 97 (4), 495–518.

Diner, D.J., et al., 2018. Advances in multiangle satellite remote sensing of speciated airborne particulate matter and association with adverse health effects: from MISR to MAIA. J. Appl. Remote Sens. 12 (4), 042603.

Dubovik, O., King, M.D., 2000. A flexible inversion algorithm for retrieval of aerosol optical properties from Sun and sky radiance measurements. J. Geophys. Res.: Atmosphere 105 (D16), 20673–20696.

Dubovik, O., Herman, M., Holdak, A., Lapyonok, T., Tanré, D., Deuzé, J., Ducos, F., Sinyuk, A., Lopatin, A., 2011. Statistically optimized inversion algorithm for enhanced retrieval of aerosol properties from spectral multi-angle polarimetric satellite observations. Atmos. Meas. Tech. 4 (5), 975.

Eck, T.F., Holben, B.N., Reid, J.S., Dubovik, O., Smirnov, A., O'Neill, N.T., Slutsker, I., Kinne, S., 1999. Wavelength dependence of the optical depth of biomass burning, urban, and desert dust aerosols. J. Geophys. Res.: Atmospheres 104 (D24), 31333–31349.

Fan, J., et al., 2018. Substantial convection and precipitation enhancements by ultrafine aerosol particles. Science 359 (6374), 411–418.

Giles, D.M., et al., 2019. Advancements in the Aerosol Robotic Network (AERONET) Version 3 database – automated near-real-time quality control algorithm with improved cloud screening for Sun photometer aerosol optical depth (AOD) measurements. Atmos. Meas. Tech. 12 (1), 169–209.

Gupta, P., Levy, R.C., Mattoo, S., Remer, L.A., Munchak, L.A., 2016. A surface reflectance scheme for retrieving aerosol optical depth over urban surfaces in MODIS Dark Target retrieval algorithm. Atmos. Meas. Tech. 9 (7), 3293–3308.

Gupta, P., Remer, L.A., Levy, R.C., Mattoo, S., 2018. Validation of MODIS 3 km land aerosol optical depth from NASA's EOS Terra and Aqua missions. Atmos. Meas. Tech. 11 (5), 3145–3159.

Holben, B.N., et al., 1998. AERONET—a federated instrument network and data archive for aerosol characterization. Rem. Sens. Environ. 66, 1–16.

Hsu, N.C., Jeong, M.J., Bettenhausen, C., Sayer, A.M., Hansell, R., Seftor, C.S., Huang, J., Tsay, S.C., 2013. Enhanced Deep Blue aerosol retrieval algorithm: the second generation. J. Geophys. Res. 118 (16), 9296–9315.

Ichoku, C., Chu, D.A., Mattoo, S., Kaufman, Y.J., Remer, L.A., Tanré, D., Slutsker, I., Holben, B.N., 2002. A spatio-temporal approach for global validation and analysis of MODIS aerosol products. Geophys. Res. Lett. 29 (12) MOD1-1-MOD1-4.

IPCC. Climate Change, 2013. In: Stocker, T.F. (Ed.), The Physical Science Basis. Contribution of Working Group I to the Fifth Assessment Report of the Intergovernmental Panel on Climate Change. Cambridge University Press, Cambridge, United Kingdom and New York, NY, USA, pp. 1535.

Kaufman, Y.J., Tanré, D., Remer, L.A., Vermote, E.F., Chu, A., Holben, B.N., 1997. Operational remote sensing of tropospheric aerosol over land from EOS moderate resolution imaging spectroradiometer. J. Geophys. Res.: Atmosphere 102 (D14), 17051–17067.

King, M.D., Kaufman, Y.J., Tanré, D., Nakajima, T., 1999. Remote sensing of tropospheric aerosols from space: past, present, and future. Bull. Am. Meteorol. Soc. 80 (11), 2229–2259.

Levy, R.C., Mattoo, S., Munchak, L.A., Remer, L.A., Sayer, A.M., Patadia, F., Hsu, N.C., 2013. The Collection 6 MODIS aerosol products over land and ocean. Atmos. Meas. Tech. 6 (11), 2989–3034.

Lyapustin, A., Martonchik, J., Wang, Y., Laszlo, I., Korkin, S., 2011a. Multiangle implementation of atmospheric correction (MAIAC): 1. Radiative transfer basis and look-up tables. J. Geophys. Res.: Atmosphere 116 (D3), D03210.

Lyapustin, A., Wang, Y., Laszlo, I., Kahn, R., Korkin, S., Remer, L., Levy, R., Reid, J.S., 2011b. Multiangle implementation of atmospheric correction (MAIAC): 2. Aerosol algorithm. J. Geophys. Res.: Atmosphere 116 (D3), D03211.

Lyapustin, A., Wang, Y., Korkin, S., Huang, D., 2018. MODIS Collection 6 MAIAC algorithm. Atmos. Meas. Tech. 11 (10), 5741–5765.

Martin, R.V., Jacob, D.J., Yantosca, R.M., Chin, M., Ginoux, P., 2003. Global and regional decreases in tropospheric oxidants from photochemical effects of aerosols. J. Geophys. Res.: Atmosphere 108 (D3), 4097. https://doi.org/10.1029/2002JD002622.

Martins, V.S., Lyapustin, A., de Carvalho, L.A.S., Barbosa, C.C.F., Novo, E.M.L.M., 2017. Validation of high-resolution MAIAC aerosol product over South America. J. Geophys. Res.: Atmosphere 122 (14), 7537–7559.

Mishchenko, M.I., Cairns, B., Hansen, J.E., Travis, L.D., Burg, R., Kaufman, Y.J., Vanderlei Martins, J., Shettle, E.P., 2004. Monitoring of aerosol forcing of climate from space: analysis of measurement requirements. J. Quant. Spectrosc. Radiat. Transf. 88 (1), 149–161.

Remer, L.A., Mattoo, S., Levy, R.C., Munchak, L.A., 2013. MODIS 3 km aerosol product: algorithm and global perspective. Atmos. Meas. Tech. 6 (7), 1829–1844.

Superczynski, S.D., Kondragunta, S., Lyapustin, A.I., 2017. Evaluation of the multi-angle implementation of atmospheric correction (MAIAC) aerosol algorithm through intercomparison with VIIRS aerosol products and AERONET. J. Geophys. Res.: Atmosphere 122 (5), 3005–3022.

Tao, M., Chen, L., Su, L., Tao, J., 2012. Satellite observation of regional haze pollution over the North China Plain. J. Geophys. Res. 117 (D12), D12203.

Tao, M., Chen, L., Wang, Z., Tao, J., Che, H., Wang, X., Wang, Y., 2015. Comparison and evaluation of the MODIS Collection 6 aerosol data in China. J. Geophys. Res.: Atmosphere 120 (14), 6992–7005.

Tao, M., Chen, L., Wang, Z., Wang, J., Che, H., Xu, X., Wang, W., Tao, J., Zhu, H., Hou, C., 2017a. Evaluation of MODIS Deep blue aerosol algorithm in desert region of east Asia: ground validation and intercomparison. J. Geophys. Res.: Atmosphere 122 (19) 10,357-310,368.

Tao, M., Wang, Z., Tao, J., Chen, L., Wang, J., Hou, C., Wang, L., Xu, X., Zhu, H., 2017b. How do aerosol properties affect the temporal variation of MODIS AOD bias in eastern China? Rem. Sens. 9 (8), 800.

Torres, O., Tanskanen, A., Veihelmann, B., Ahn, C., Braak, R., Bhartia, P.K., Veefkind, P., Levelt, P., 2007. Aerosols and surface UV products from Ozone Monitoring Instrument observations: an overview. J. Geophys. Res. 112 (D24), D24S47.

Wang, J., Xu, X., Spurr, R., Wang, Y., Drury, E., 2010. Improved algorithm for MODIS satellite retrievals of aerosol optical thickness over land in dusty atmosphere: implications for air quality monitoring in China. Rem. Sens. Environ. 114 (11), 2575–2583.

Xu, X., Wang, J., 2015. Retrieval of aerosol microphysical properties from AERONET photopolarimetric measurements: 1. Information content analysis. J. Geophys. Res.: Atmosphere 120 (14), 7059–7078.

Xu, X., et al., 2015. Retrieval of aerosol microphysical properties from AERONET photopolarimetric measurements: 2. A new research algorithm and case demonstration. J. Geophys. Res.: Atmosphere 120 (14), 7079–7098.